Review

Interfacial pre-transmembrane domains in viral proteins promoting membrane fusion and fission

Maier Lorizate [1], Nerea Huarte, Asier Sáez-Cirión [2], José L. Nieva *

Unidad de Biofísica (CSIC-UPV/EHU), Universidad del País Vasco, Aptdo. 644, 48080 Bilbao, Spain
Departamento de Bioquímica y Biología Molecular, Universidad del País Vasco, Aptdo. 644, 48080 Bilbao, Spain

Abstract

Membrane fusion and fission underlie two limiting steps of enveloped virus replication cycle: access to the interior of the host-cell (entry) and dissemination of viral progeny after replication (budding), respectively. These dynamic processes proceed mediated by specialized proteins that disrupt and bend the lipid bilayer organization transiently and locally. We introduced Wimley–White membrane-water partitioning free energies of the amino acids as an algorithm for predicting functional domains that may transmit protein conformational energy into membranes. It was found that many viral products possess unusually extended, aromatic-rich pre-transmembrane stretches predicted to stably reside at the membrane interface. Here, we review structure–function studies, as well as data reported on the interaction of representative peptides with model membranes, all of which sustain a functional role for these domains in viral fusion and fission. Since pre-transmembrane sequences also constitute antigenic determinants in a membrane-bound state, we also describe some recent results on their recognition and blocking at membrane interface by neutralizing antibodies.
© 2007 Elsevier B.V. All rights reserved.

Keywords: Viral membrane fusion; Viral membrane fission; Fusion peptide; Pre-transmembrane; MPER; Peptide–lipid interaction; HIV-1 gp41; WW scale

Contents

1. Introduction

Membrane fusion and fission can be considered as energetically unfavorable reactions that involve hundreds of lipid molecules with no change in covalent bonding. These complex physiological reactions proceed coupled to the basic processes of local rupture (exposure of the hydrophobic interior) and deformation (bending) of lipid bilayers (reviewed in Refs. [1,2]). Enveloped animal viruses rely on the fusogenic activity of membrane integral surface glycoproteins to enter and infect their host-cells [3–7], while fission is required for pinching-off of newly assembled virions [1]. Membrane fission is also operational intracellularly all along virus infectious cycles [8]. For example trafficking of viral proteins during assembly at the plasma or intracellular membranes and perhaps during intracellular translocation of the capsid complexes is dependent on this process [9].

Fusion protein machinery delivers energy in order to perform a series of jobs, including bringing the membranes into close contact and the sequential formation of only-lipid ("stalks") and lipid-aqueous connections ("fusion pores") [10–14]. Although these proteins share little sequence homology even between members of the same family, evolutionary convergence has produced a number of common features [1,7,12]: functional priming at the cell surface through proteolytic processing, oligomeric organization (homotrimers of heterodimers in most cases), activity localized into ecto and transmembrane domains of the integral subunit, and the presence of a fusion peptide (FP), a highly conserved, hydrophobic domain, usually located at or close to the free amino-terminus of the integral subunit.

Viral fusogenic function, on the other hand, has been assembled within two structurally divergent scaffolds [4,12,15]. Class I fusion proteins are all characterized by their capacity to fold into a highly stable 6-helix bundle (6-HB). In this "hairpin-like" trimeric structure three helices pack in the reverse direction against hydrophobic grooves outside a triple-stranded coiled-coil, so that the ectodomain amino- and carboxy-termini are placed at the same end of the molecule. It is generally thought that amino-terminal FP sequences insert into the target cell membrane in a "pre-hairpin" stage [16–18]. Subsequent production of the 6-HB would therefore induce close apposition of the viral and cell membranes anchored through the transmembrane domain (TMD) and the FP, respectively. In contrast, class II proteins are composed of antiparallel β-sheet structures and possess internal FPs [4,12,15,19]. Despite these differences, class II proteins have evolved into structures capable of triggering fusion following a mechanism essentially similar to that of class I proteins [15,19], namely, FP insertion into the target

membrane and folding into a low-energy trimer that brings into contact TMD- and FP-anchored membranes.

Thus, protein conformational energy, such as that released upon 6-HB formation, must be coupled with membrane merger by means of membrane-inserting specialized domains. In this review we will not address the FPs, since these force-transmitting domains, together with additional assistant elements scattered along the ectodomain sequences, have been recently subject of thorough revision in these series [17,18,20]. Here, we will specifically focus on the domains that precede transmembrane anchors in viral proteins promoting fusion–fission. These sequences have been defined as distinct domains according to their tendency to partition from water into the membrane interface (designated as "pre-transmembrane" domains, PreTM), and also attending to its implication in fusion and viral neutralization processes (designated as "membrane-proximal external regions", MPER).

Since a hydrophilic, flexible, structurally irregular PreTM linker might keep the 6-HB far from the close contacting dehydrated areas required for membrane fusion initiation (as far as 70Å apart from the viral membrane in the case of HIV), it has been argued that force transmission requires the establishment of contacts between this element and the viral membrane [21]. Moreover, the proximal location of PreTM covalently linked to TMD ensures the high effective concentrations favoring its insertion into membranes. Accordingly, the capacity of PreTM regions for inserting into membranes has been extensively studied in model vesicular systems using representative synthetic peptides. These studies further suggest a putative role of membrane-inserted PreTMs as promoters of lipid bilayer destabilization. In the following sections we review experimental results, obtained in different viral systems, all of which sustain the functional activity of viral PreTMs in fusion–fission, either by transmitting protein conformational energy into membranes, and/or by perturbing lipid bilayer integrity.

2. Hydrophobicity-at-interface: a tool for unraveling viral PreTM sequences

In previously published review work we described the application of Wimley–White (WW) scales to the detection of viral sequences that show tendency to partition into membrane interfaces [22]. The analysis was performed with the premise that glycoprotein globular ectodomains behave as non-constitutive membrane proteins, i.e., initially soluble species capable of inserting spontaneously into uncharged cell target membranes in the course of the fusion process. Wimley and White calculated the water-to-membrane interface transfer free energies for each amino acid in the context of unfolded peptide
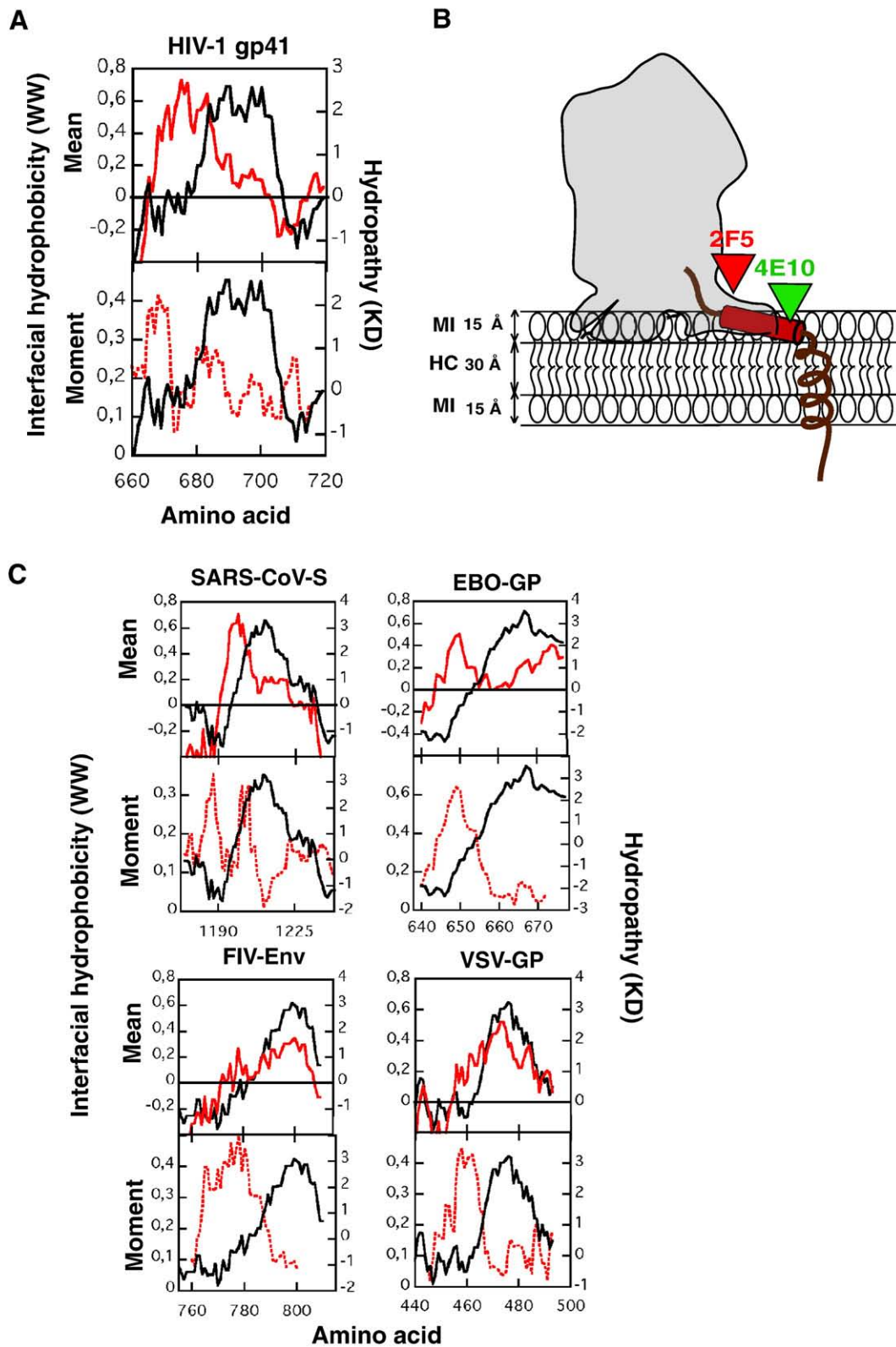
Fig. 1. Interfacial PreTM domains in viral fusion proteins as predicted by the combined WW–KD hydrophobicity analysis. A) Membrane-proximal external and transmembrane regions of HIV-1 gp41. Hydropathy (mean values for a window of 11 amino acids) was plotted according to the Kyte–Doolittle hydropathy index (black lines), Wimley–White interfacial hydrophobicity (top panel, red-continuous trace) or Wimley–White interfacial moment (bottom panel, red-dotted line). B) Predicted location of gp41 AIS-PreTM (red cylinder) at the viral membrane interface. The cryoET density map contour of SIV envelope spike is indicated by the gray surface [36]. C) Analyses of membrane-proximal external and transmembrane regions in selected examples.

chains (ΔG_{wiu}-s) [23,24]. These free energy values were postulated as a hydrophobicity scale that compiles the energetic components dictating initial partitioning of sequences into membranes, specifically when this occurs in the absence of repulsive or attractive electrostatic interactions. As compared to classical hydropathy indexes based on bulk-phase partitioning of side chain alone, WW "interfacial hydrophobicity scale" takes into account the effect of the membrane interface on partitioning and includes the energy cost of peptide bond partitioning into it. This originates important differences in residue hydrophobicities, aromatic residues, namely Phe, Tyr and Trp, appearing to be the most hydrophobic ones when located at membrane interfaces.

Hydrophobicity-at-interface WW scale was first applied to HIV-1 and Ebola FPs with the aim of confirming their tendency to spontaneously partition from water into the bilayer interface [25–27]. Features of HIV-1 and Ebola FP sequences as potential membrane anchors were readily evident upon Kyte–Doolittle (KD) hydropathy analysis [28]. Thus, KD and WW hydropathy plots displayed positive peaks coincident with the FP sequences. However, a further analysis combining both scales disclosed segregated peaks at the membrane-proximal region of HIV-1 gp41 ectodomain (Fig. 1A and Refs. [29,30]). When compared to the KD peak spanning gp41 TMD, the positive maximum detected by WW was shifted 15–20 residues towards the N-terminus (continuous red plot in top panel of Fig. 1A). The combined WW–KD analysis thus suggested the existence of a wide nonpolar region (approximately 40–50 residues long) at the C-terminus of the gp41 ectodomain (Table 1). This region would be segmented into two domains: one, positioned somewhat farther from the protein C-terminus (residues 664–683 in HIV-1), which would remain stably inserted within the membrane interface (designated as PreTM [29]), and another one located closer to the C-terminus that constitutes the TMD.

Further development of the WW analysis included the calculation of the hydrophobic-at-interface moment [21,31]. Hydrophobic moments measure the periodicity of residue distribution along the secondary structure elements [32,33]. Preferential orientation of the hydrophobic residues towards one face of the structure element has been proposed to favor hydrophobic interactions between protein structural components and between membranes and protein sequences. Computation of the hydrophobic moment using the membrane interface-to-water transfer free energies (ΔG_{iwu}) for each amino acid [23] suggested that

gp41 PreTM can be elongated at the N-terminus to include a stretch whose face shows strong affinity for membranes, if folded into an α-helix (Fig. 1A red-dotted plot in bottom panel). It must be noted that this amphipathic-at-interface stretch could not be detected when KD or Eisenberg scales were used [21]. Moreover, the moment peak shown in Fig. 1A (bottom panel) was present in different HIV-1 isolates and in other lentiviruses thereby suggesting that the N-terminal segment of gp41 PreTM consists in a conserved amphipathic-at-interface sequence, recently designated as AIS [34].

In summary, the hydrophobicity analysis in Fig. 1A predicts the existence of a gp41 region anchored to the viral membrane through an interfacial sequence, amphipathic at its N-terminus, which is followed by the fully hydrophobic transmembrane helix (Table 1 and cartoon in Fig. 1B). The physiological relevance of gp41 AIS-PreTM-TMD motif has recently received support from structural studies in intact SIV and HIV virions [35,36]. Cryoelectron microscopy tomography has disclosed stalk regions that project as "legs" from the trimeric Env complex, with their "feet" just above the plane of the envelope (tripod-like structure, contour in Fig. 1B) [36,37]. This observation would be consistent with native Env AIS-PreTM monomers being located at the viral surface, and inserted in parallel to the external membrane monolayer plane.

Extension of WW analysis to envelope spikes of several virus families suggests that an interfacial location of membrane-proximal external regions might be a common structural feature [29,38]. Fig. 1C and Table 1 provide several examples that illustrate different outcomes of the combined WW–KD hydrophobicity analysis. The presence of a hydrophobic-at-interface, aromatic-rich sequence within the fusogenic S2 subunit of SARS coronavirus spike S was already reported [39,40]. The analysis in Fig. 1C adds to this finding the existence of a pattern similar to that previously described for HIV-1 gp41 (panel A). The plots thus indicate that the fully hydrophobic-at-interface SARS S2 PreTM sequence can be elongated at the N-terminus to include an amphipathic-at-interface stretch (see also Table 1). A comparable but different situation occurs in the case of the Ebola fusion protein. Ebola GP contains within the membrane-proximal region of the GP2 ectodomain an approximately 10aa-long sequence showing a high tendency to partition into membrane interfaces (Ref. [31], see also Table 1). However, computation of the hydrophobic-at-interface moment for this element reflects the existence of a longer amphipathic-at-

Table 1
AIS-PreTM-TMD motifs in selected examples of viral fusion proteins

Protein [a]	Sequence [b]
HIV-1 Env	658-QELLELDK**WASLWNWFNITNWLWYIK***LFIMIVGGLVGLRIVFAVLSVV*NR-707
SARS Co-S	1181-DLQELGKYEQ**YIKWPWYVWLGFIAGLIAI***VMVTILLCCMTSCCSCL*-1226
Ebola GP	639-GDND**NWWTGWRQWI**PA*GIGVTGVIIAVIALFCICKFVF*-676
FIV Env	760-GKTGIQQLQKWEDWVRWIGNIPQYLK*GLLGGILGIGLGVLLLILCLPTLV*D-810
VSV-GP	449-NPIDFVEGWFS***SWKSSIASFFFIIGLIIGLFLVLRVGIYLYI***KLK-493

[a] Numbering based on the HIV-1 HXB2, Ebola Zaire, FIV Petuma, SARS-CoV Urbani and VSV Indiana, strains/serotypes.

[b] Sequences in boxes and bold span, amphipathic-at-interface and hydrophobic-at-interface domains, respectively, as determined by WW algorithm. Underlined sequences in italics denote hydrophobic transmembrane sequences estimated according to KD algorithm. The range of each sequence has been inferred from plots displayed in Fig. 1.

interface sequence that would span over ca. 17 amino acids (Table 1).

Finally, the retroviral FIV Env and vesiculoviral VSV-GP spike sequences serve to illustrate an additional case. Both PreTMs are characterized by negligible mean interfacial hydrophobicity. The presence of several conserved Trp-s within fusogenic FIV gp36 subunit's membrane-proximal sequence was previously noted [41,42]. These hydrophobic-at-interface residues are inter-dispersed with helical periodicity by charged residues that bear the lowest tendency to partitioning into membrane interfaces (Table 1). Similarly, aromatic residues at the VSV G PreTM are intervened by stretches with low propensity for partitioning (Table 1 and Ref. [43]). As a result, in both cases the mean hydrophobicity is low and interfacial mo-

ment high, reflecting a propensity for interfacial insertion, but only upon PreTM folding as an α-helix.

In what follows we summarize a series of experimental results that sustain the involvement of the predicted interfacial PreTM domains in membrane-rearrangements leading to viral fusion–fission.

3. Structure–function studies of HIV-1 gp41 PreTM

3.1. Mutational analyses

Mutational analysis of gp41 MPER by Salzwedel and co-workers [44] provided compelling evidence to support PreTM involvement in HIV-1 fusion. Deletion of the entire PreTM
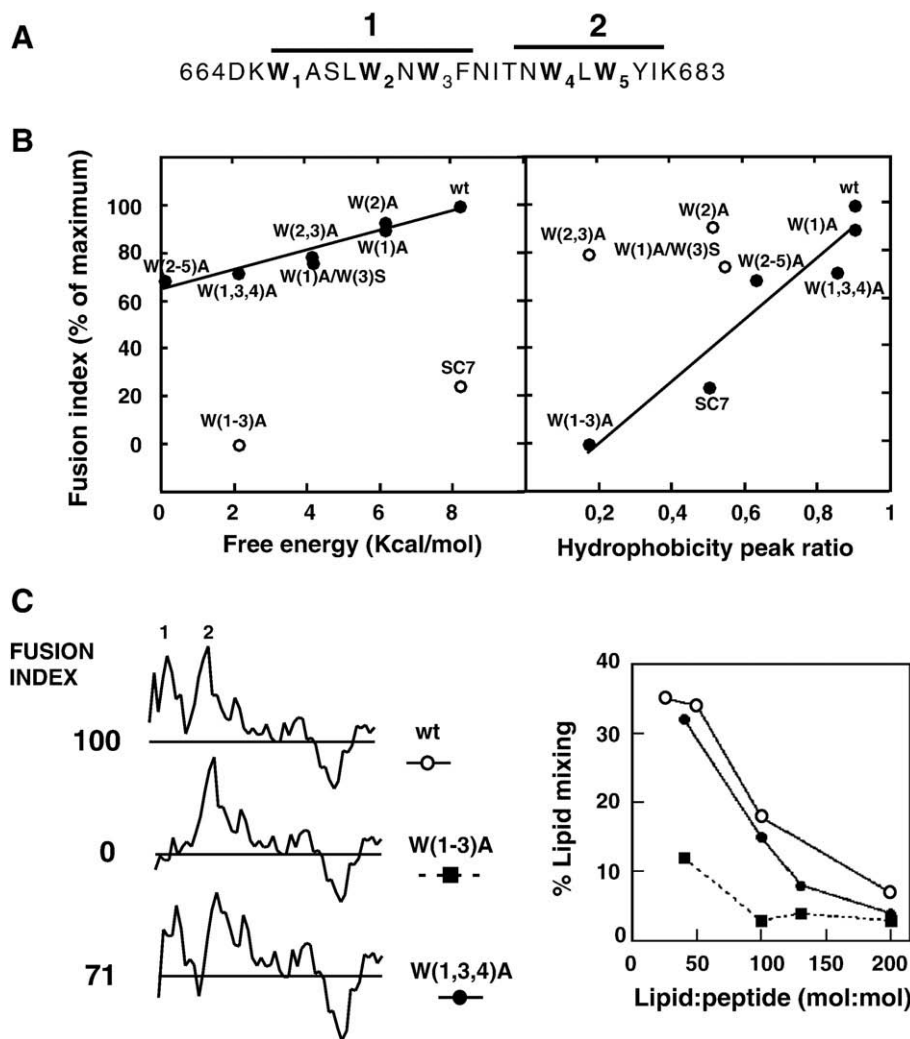
Fig. 2. Hydrophobicity-at-interface analysis of gp41 PreTM mutants. A) Gp41 PreTM sequence. Mutated Trp residues are in bold. Bars on top span the two interfacial domains disclosed when mean hydrophobicity values are calculated for a window of 5 amino acids (see panel C). B) Correlation between PreTM overall free energy of partitioning (left) or peak intensity ratio (right) and fusogenicity (average number of syncytia in the field as reported by Salzwedel et al. [44]). Plotted values in right panel correspond to peak 1/peak 2 intensity ratios as obtained from hydropathy-at-interface plots similar to that displayed in panel C. In both panels hollow symbols indicate values not correlating with the represented linear regressions. C) Effect WW hydrophobicity distribution on PreTM function. Left: Hydropathy-at-interface plots (window of 5 amino acids) for the PreTM-TMD regions (amino acids 660–720 in Env precursor) derived from the wild-type and mutants W(1,3,4)A and W(1–3) A. Fusion index as in previous panel. Right: Membrane fusion induced in a vesicular system by DKWASLWNWFNITNWLWYIK (empty circles), DKAASLWNAFNITNALWYIK (black circles) and DKAASLANAFNITNWLWYIK black squares) peptides, representing PreTM regions of gp160 wt, W(1,3,4) A and W(1–3)A mutants, respectively. Final extents (percentages after 30 min) of intervesicular mixing of lipids were determined as a function of the peptide-to-lipid mol ratios in 1-palmitoyl-2-oleoylphosphatidylcholine:cholesterol (1.5:1) vesicles.

(Δ665–682) abrogated the ability of the envelope glycoprotein to mediate cell–cell fusion without affecting the normal maturation, transport, or CD4-binding ability of the protein. This fusion phenotype was also demonstrated for W(1–5)A, a PreTM mutant devoid of interfacial hydrophobicity by substituting alanine residues for the five tryptophan residues within this sequence. Further analysis using a three-color cell–cell fusion assay [45] confirmed that gp41 lacking PreTM is incapable of mediating both membrane-and-volume mixing. Interestingly, the fusion induced by W(1–5)A mutant was blocked at the stage of non-expanding small fusion pores. This activity is similar to that exhibited by GPI-linked hemagglutinin (GPI-HA) of influenza virus [46].

We applied interfacial hydrophobicity to the analysis of the numerous mutations generated by Salzwedel and co-workers (Fig. 2 and Ref. [21]). Hydropathy plots of mean values calculated for a sliding window of 5 amino acids displayed two defined positive peaks, consistent with a slightly longer PreTM that encompasses two segregated interfacial subdomains (Fig. 2). The N-terminal peak was found to span the conserved amphipathic-at-interface helix or AIS domain [34]. We observed that a number of blocking deletions invariably correlated with the ablation and/or merging of interfacial subdomains [21]. An extension of this analysis is displayed in Fig. 2B. Overall free energy of partitioning (left) and interfacial hydrophobicity distribution (right) was plotted vs. fusogenicity of N-terminal subdomain Ala mutants. Free energy of partitioning, computed as the sum of the free energies of the constituent amino acids, correlated linearly with activity of most substitution mutants, but displayed significant activity for $\Delta G_{iwu} = 0$, indicating that favorable PreTM partitioning into membranes contributes to, but is not essential for gp41-mediated fusion. In addition, partitioning free energy cannot account for the fusion-inhibitory effects of scrambled SC7 and W(1–3)A mutations (hollow symbols). The effect of these mutations on function seems to better correlate with distribution of hydrophobicity into two subdomains (right panel). When hydrophobicity-at-interface peak ratios were plotted vs. fusogenicity, a positive correlation was observed for these and other mutants. This observation supports the functional relevance of distributing interfacial hydrophobicity into two segregated subdomains.

A remarkable example of interfacial hydrophobicity distribution effect is that of W(1–3)A and W(1,3,4)A substitutions, only differing in the position of one Trp residue (Fig. 2C). While

the former mutation abolished gp41-induced fusion, the latter maintained ca. 70% of wild-type activity. The hydropathy plots revealed the effect of these mutations on hydrophobicity distribution (left panel). Whereas W(1,3,4)A mutant retained two hydrophobic-at-interface segments, W(1–3)A showed a single interfacial domain (left panel). Panel C compares the fusogenic
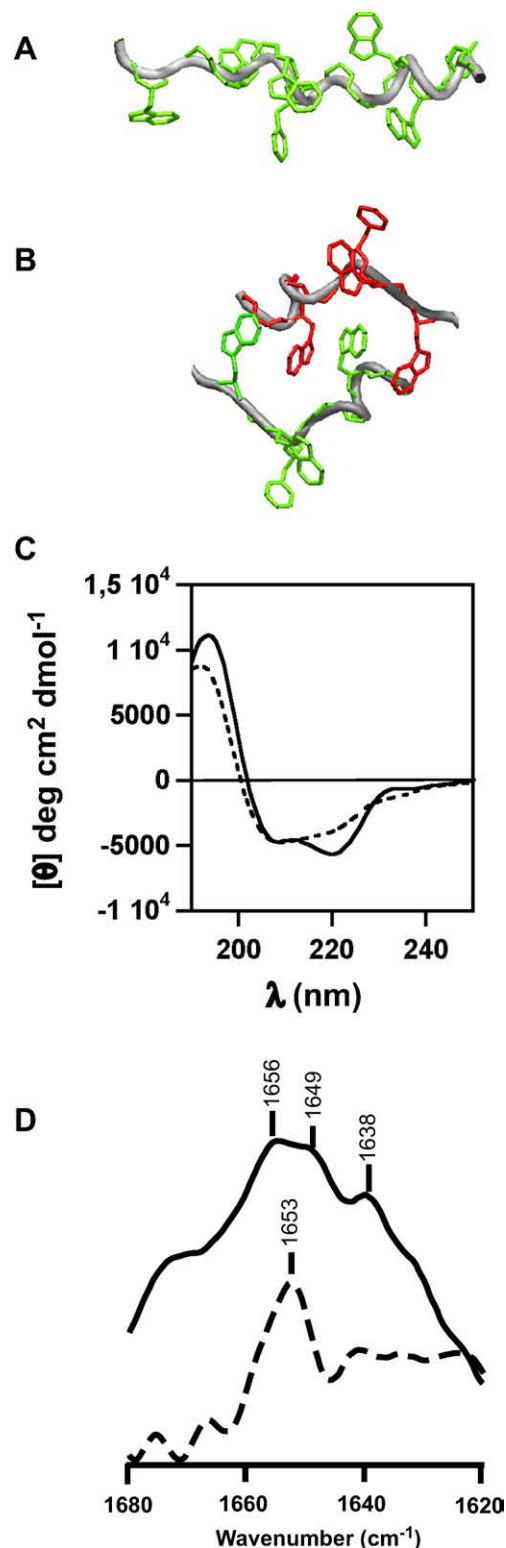
Fig. 3. Structural features of gp41 PreTM. A) NMR structure of KWASLWNWF-NITNWLWYIK in DPC micelles [49] (PDB entry: 1JAU). Aromatic side chains are displayed. B) X-ray structure of KGWNWFDITNWGK peptide bound to Fab 4E10 [50] (PDB entry: 1TZG), 2 peptides displaying aromatic side chains have been oriented to show the interaction in the crystal unit cell. C) CD spectra of PreTM$_p$ (DKWASLWNWFNITNWLWYIK) in DPC (5 mM) micelles (dotted) and POPC vesicles (continuous trace). Lipid-alone signal was subtracted from these samples. D) Fourier self-deconvolved infrared spectra of PreTM$_p$ incorporated into POPC membranes. The peptide was added to vesicles at 1:50 and 1:1000 peptide-to-lipid mol ratios, top and bottom spectrum, respectively. Lipid–peptide complexes were subsequently isolated from the floating fractions after ultracentrifugation in D$_2$O buffer. The spectra are not drawn to the same scale to better show the 1680–1620 cm^{-1} amide I region. Structures in panels A and B were rendered with the Swiss-PDB-viewer program.

activities of peptides representing these sequences (PreTM$_p$-s) in a lipid vesicle system. The peptide corresponding to the fusion-competent W(1,3,4)A phenotype was as efficient as the wild-type peptide in fusing lipid vesicles. In comparison, the peptide representing the fusion-defective W(1–3)A phenotype displayed lower activity. Thus, fusion measured in a vesicular system suggests that the observed fusion W(1–3)A phenotype might reflect this mutant's incapacity to induce membrane-restructuring.

3.2. Structural studies

In accordance with the TMD paradigm, PreTM is postulated to fold within the low-polarity membrane interface environment adopting a helical conformation [24,47], but also self-aggregate therein [48]. Structural studies support both possibilities (Fig. 3). NMR spectroscopy revealed the formation of a well-defined helical structure for KWASLWNWFNITNWLWYIK peptide monomers in dodecylphosphocholine micelles (panel A and Ref. [49]). Four of the five tryptophan residues, as well as the tyrosine residue, formed a "collar" of aromatic residues along the axial length of the helix. Nuclear Overhauser effects to the headgroup and interfacial protons of protonated dodecylphosphocholine confirmed that the aromatic residues are positioned within the membrane-water interface of a phospholipid bilayer sustaining a "Velcro-like" interaction. The bulk of the polar residues is positioned on one face of this structure, with the hydrophobic phenylalanine side chain on the opposing face, forming an amphipathic structure.

An additional PreTM atomic structure was obtained from the resolution of Fab 4E10 (see below) in complex with KGWNW-FDITNWGK peptide (panel B and Ref. [50]). The bound peptide also adopts a helical conformation in which residues contacting the paratope, W672, F673, I675, and T676, map to one face of the helix. Interaction of two peptide chains in the unit cell shows

the close interdigitation of W670 and W678 indole side chains. Dimers perhaps mimic a low-energy conformation in the intact gp41 oligomer or reflect a biologically important interaction of the peptide Trp residues with the viral membrane [50].

Low-resolution structural techniques provide evidence for the existence of monomeric and multimeric PreTM states in a membrane environment (panels C and D). CD helical spectrum of monomeric PreTM$_p$ in DPC micelles displayed a $[\theta]_{222}/[\theta]_{208}$ ratio < 1 (dotted trace in panel C, see also Ref. [49]). By comparison, CD spectrum of PreTM$_p$ incorporated into PC vesicles at a 1:33 peptide-to-lipid mol ratio (continuous trace) resulted in an increase of the intensity of the positive peak together with a $[\theta]_{222}/[\theta]_{208}$ ellipticity ratio > 1, which supports the existence of helix–helix interactions such as those described for heterodimeric coiled-coils and/or transmembrane helical bundles [51–53]. Fluorescence data indeed indicated that rhodamine-labeled PreTM$_p$ in lipid vesicles self-associates at the doses used to carry out these measurements [21,54] (see also Fig. 4).

IR spectroscopy confirmed the presence of helical structures as both, monomers or multimers in PC membranes (panel D and Ref. [21]). At the peptide-to-lipid ratio of 1:1000, where the peptide is most likely monomeric according to the rhodamine fluorescence data, PreTM$_p$ spectrum showed a symmetrical band at 1653 cm^{-1} consistent with a canonical α-helix (Fig. 5B). At the 1:50 ratio where self-association is prominent, the α-helical band splitted into two components, absorbing at 1656 and 1649 cm^{-1}, besides the presence of a band at 1639 cm^{-1}, as was postulated previously for coiled-coils [55]. Thus, combined CD and IR structural data are compatible with the existence of a monomeric helical structure, prevalent in membranes at low doses, which would self-associate with increasing membrane loads.

Finally, it is important to note that the mutagenesis studies by Salzwedel et al. did not support the requirement of helical
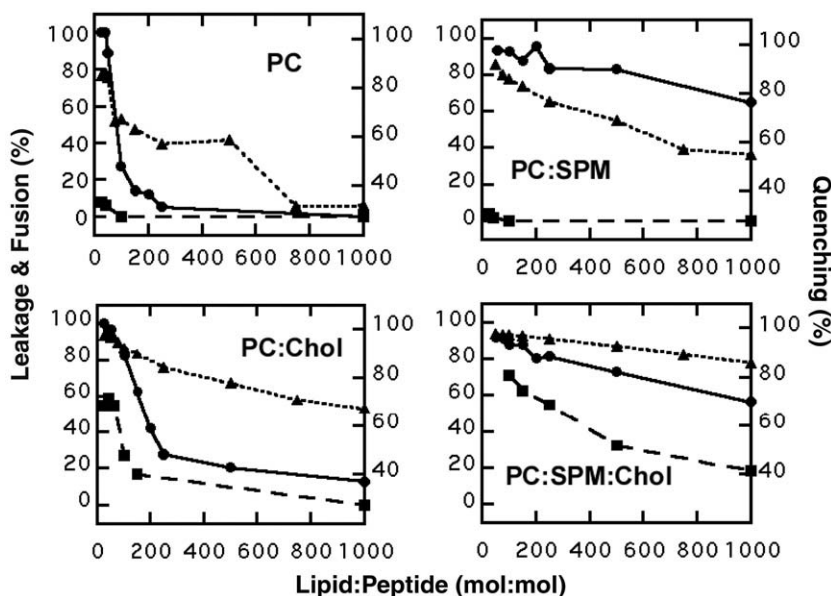
Fig. 4. HIV-1 gp41 PreTM$_p$ surface aggregation and correlation with induced membrane-restructuring in lipid vesicles of different composition. The percentage of Rho-PreTM$_p$ quenching (triangles and dotted lines) and PreTM$_p$-induced leakage (circles and continuous lines) and lipid-mixing (squares and dashed lines) after 30 min of incubation with vesicles was plotted as a function of the lipid-to-peptide mol ratio. Final lipid concentration was 100 μM in all cases.
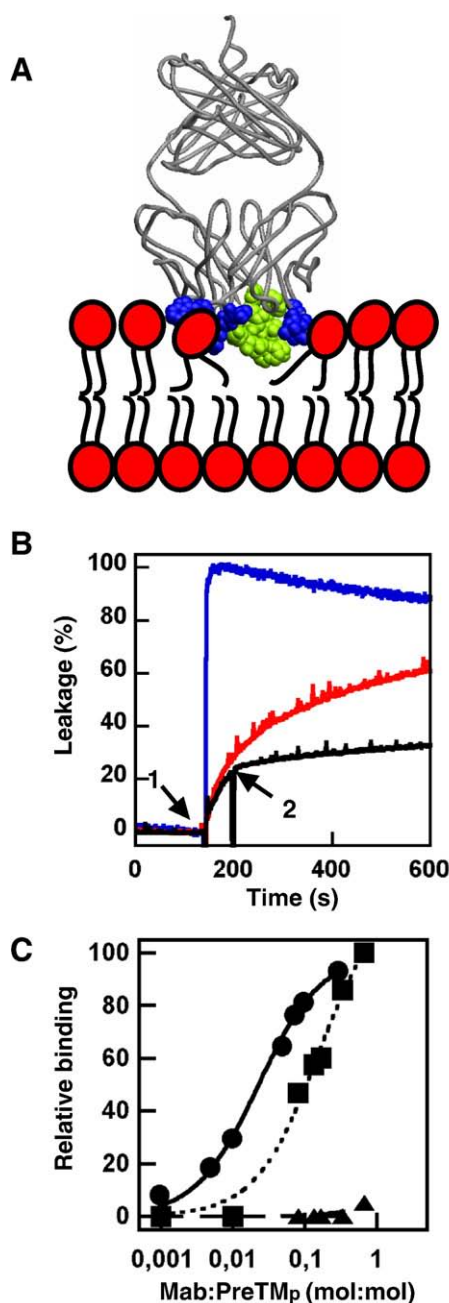
Fig. 5. Inhibition of HIV-1 gp41 PreTM$_p$-induced membrane-restructuring by Nab 4E10. A) Model for epitope recognition at the membrane interface by Fab 4E10 (Solid ribbons). Space-filled atoms in blue denote hydrophobic-at-interface residues exposed to solvent in CDR H2 and H3 loops. Atoms in green belong to bound KGWNWFDITNWGK peptide. Structure, derived from 1JAU PDB entry, was rendered with the Swiss-PDB-viewer program. B) Inhibition of ongoing ANTS leakage with Mab4E10. POPC:Chol (2:1) LUV suspensions (100 μM lipid) were treated with 1 μM PreTM$_p$ (arrow 1) and, further supplemented (arrow 2) with 25 μg/ml of Mab4E10 (black traces). Controls in absence of antibody are in red. Blue traces correspond to dansyl fluorescence increase (arbitrary units) upon PreTM$_p$ addition. Adapted from Fig. 3 in Ref. [103]. C) Recognition of PreTM$_p$ bound to ELISA plaques (circles), PC:Chol vesicles (squares) and PC:SPM vesicles (triangles). Inhibition percentages (Leakage) or percentages of maximal binding (ELISA) were plotted as a function of Mab4E10 binding site-to-PreTM$_p$ mol ratio (i.e., 2 binding-sites per Ma4E10 molecule).

conformations in the function of this region [44]. The potential role of an α-helical PreTM structure in fusion was tested by deleting two central nonconserved residues, or substituting W672 for with proline. These mutations that would destabilize an α-helical conformation were found to have no significant effect on gp41 function, therefore arguing against a topological requirement for a helical structure. However, the reduction of the fusogenicity of the glycoprotein observed after scrambling PreTM central residues (mutant SC7) suggests that the clustering of hydrophobic residues in an α-helical secondary structure may indeed be important, but not essential, for the function of this region.

3.3. Membrane interactions of representative peptides

Early definition of HIV-1 gp41 PreTM as a membrane-inserting domain prompted the comparison of synthetic DKW-ASLWNWFNITNWLWYIK (PreTM$_p$) and AVGIGALFLGF-LGAAGSTMGARS (FP$_p$) in their capacities for perturbing membranes [29,30]. These studies were conducted under the assumption that PreTM might represent a second FP, i.e., an additional domain participating in the induction of the viral membrane perturbations required for fusion. Sustaining this notion, lower doses of PreTM$_p$ were required to induce fusion and permeabilization of liposomes [29,30]. Moreover, PreTM$_p$-induced restructuring effects were modulated by the main lipids existing in the viral envelope (Fig. 4 and Ref. [54]). Aloia and co-workers [56,57] found in HIV-1 membranes increased Chol-to-phospholipid molar ratios and high levels of sphingomyelin (SPM), ca. 2–3 times that of the host-cell surface membranes. These findings were subsequently confirmed using a lipidomic approach [58]. It is therefore assumed that the HIV-1 membrane is enriched in Chol and SPM, an observation that correlates with the virion selectivity for specific segregated membrane regions through which virions emerge during maturation [59].

Results displayed in Fig. 4 illustrate the effect of these lipids on PreTM$_p$-induced leakage and fusion of liposomes. PreTM$_p$ induced leakage from pure PC liposomes at high peptide-to-lipid ratios (ca. >1:100 mol:mol) concomitant to an increase in its self-aggregation, as revealed by an increase in the quenching level of Rhodamine-labeled species from approximately 40 to 80% (PC labeled panel). No significant fusion could be detected even at the highest doses tested, namely 1:10. Under conditions that did not significantly affect partitioning, inclusion of SPM or Chol in POPC membranes had dissimilar effects. SPM sustained the formation of lytic pores even when Rhodamine indicated quenching levels below 60% (PC:SPM panel). In contrast, Chol promoted fusion activity under self-aggregation levels (60–80% rhodamine quenching) also inducing leakage (PC:Chol panel). A similar Chol-dependence for PreTM$_p$-induced vesicle–vesicle fusion was found in experiments comparing PreTM$_p$ with longer derivatives [60].

When the three lipids were combined (PC:SPM:Chol panel) to emulate conditions putatively existing at the external membrane monolayer of HI virion, high levels of self-aggregation (rhodamine quenching >80%), concomitant to an enhancement in fusion and lytic activities were observed at low doses (in the

order of 1:1000 peptide-to-lipid ratio). Conditions described to disturb occurrence of lateral separation of s_0–l_0 lipid phases in these systems, reproduced the high peptide-dose requirements for leakage as found in pure POPC vesicles and inhibited fusion [54]. In summary, the quenching efficiency data as a function of the peptide-dose in LUV suggests that indeed peptide-aggregates are involved in membrane perturbations, and that s_0–l_0 phase-coexistence promotes PreTM clustering at the mol ratios existing in the HI virion envelope. Thus, these results support the notion that the PreTM domain aids in the clustering of gp41 within the HIV-1 envelope, and in destabilization of the bilayer architecture at the loci of fusion.

The existence of a direct interaction between Chol and PreTM domain was already posited by Salzwedel et al. [44]. PreTM carboxy-terminal LWYIK sequence was later identified as a potential "cholesterol recognition/interaction amino acid consensus" (CRAC) by measuring the binding to cholesterol of a series of gp41-derived sequences fused to maltose binding protein [61]. Recently reported experimental evidence and modeling studies provide the physicochemical grounds for a direct interaction of PreTM-CRAC with Chol [62–64]. PreTM–Chol interaction would be based on two capacities of CRAC sequence, namely, wrapping and blocking of the interfacial cholesterol OH group by H-bond interactions, and stacking of aromatic side chains with A ring of cholesterol. This interaction model has been proven through site-directed mutagenesis [63]. A conservative L679I substitution, which otherwise reduces the interaction of CRAC-representative peptides with Chol, result-ed in a significant attenuation of Env fusogenicity measured in a cell–cell fusion assay. Thus, these results established a direct link between capacity to bind Chol-rich domains and biological activity.

In conjunction, vesicle perturbation assays and calorimetry determinations suggest that a PreTM–Chol complex might form at the interface of the external viral membrane monolayer with the potential of inducing membrane perturbations upon self-assembly [54,62,63]. However, as discussed by Epand [64], the fact that L679I mutation did not completely abolished gp41 function posits the possibility that a fraction of the fusion activity measured in cells is not dependent on PreTM–Chol interactions. Sustaining the notion that Chol-dependent mem-brane perturbations induced by PreTM are not absolutely required for gp41-induced cell–cell fusion, an Env construct bearing FP blocking mutation and functional PreTM did not destabilize the plasma membrane upon receptor/co-receptor engagement [65]. Conversely, activated Env with functional FP but deleted PreTM was able to permeabilize the plasma mem-brane of expressing cells.

4. Studies on viral PreTM domains involved in membrane fusion

A PreTM domain detected within gp36 fusogenic subunit has been suggested to play a functional role in FIV entry [41,42,66]. A synthetic peptide modeled on such motif inhibited FIV replication very efficiently, most likely by blocking entry [66]. In a later report, 11 mutated clones having the Trp-rich

motif scrambled or variously deleted or substituted were pro-duced and evaluated in their capacity of infecting susceptible cells [41]. The functional effects of conserved Trp mutations were analyzed on assembled virions. The viral particles gene-rated by the constructs having the Trp motif deleted, scrambled, or Ala substituted at two or three Trp positions were indeed replication-incompetent. In the latter mutants infection was re-stored by providing an independent source of intact FIV envelope glycoproteins or by addition of the fusing agent poly-ethylene glycol, thus indicating that their defect resided pri-marily at the level of cell entry. The fact that FIV PreTM was functionally active in fusion was supported by results of another site-directed mutagenesis study [42]. In this case, the W(1–3)A Env protein showed similar levels of expression and processing as the wild-type, but was completely defective in forming syn-cytia. It was concluded that this region must be critical for fusion by FIV Env and that the presence of tryptophans is required for this property.

The high degree of conservation observed upon sequence alignment of envelope glycoprotein (G) MPERs from several different vesiculoviruses suggested that PreTM might be also important for VSV G function. This was confirmed by Whitt and co-workers [43,67,68] who showed the involvement of this domain in VSV fusion and budding (see next section). Deletion of the 13 stem amino acids (N449 to W461) that span the VSV AIS domain (Table 1) dramatically reduced cell–cell fusion activity and reduced virus infectivity approximately 100-fold [43]. However, mutation of conserved aromatic residues res-ponsible for amphipathicity (W457, F458, and W461) either singly or together had only modest effects on cell–cell fusion activity. Notably, PreTM-TMD-cytoplasmic tail constructs (GS) expressed in cells could also potentiate the membrane fusion activity of heterologous viral fusion proteins [68]. For some fusion proteins, there was as much as a 40-fold increase in syncytium formation when GS was coexpressed compared to that seen when the fusion protein was expressed alone. Fusion potentiation by GS was not protein specific, since it occurred with both pH-dependent as well as pH-independent fusion proteins. Truncation mutations indicated that the complete VSV AIS was required for fusion potentiation. Together, these data support the hypothesis that the PreTM domain contributes to VSV G-mediated membrane fusion activity and functions as a fusogenic unit, yet the conserved aromatic residues seem to be not essential for membrane fusion or infectivity in the context of the assembled virus.

The membrane interactions of Ebola PreTM$_p$-s, studied in a vesicular system, supported the involvement of Ebola G PreTM in membrane fusion (Fig. 1 and Ref. [31]).Thus, DNDNWW-TGWRQWIPAGIG and DWGDAPNWRWNWGIIGTQ, repre-senting the Ebola glycoprotein PreTM or a "scrambled" control with a different hydrophobic-at-interface moment, respectively, were characterized in a study that combined the assessment of insertion into lipid monolayers, changes in intrinsic fluores-cence and infrared spectroscopy [31]. Only the former bound the membrane interface under equilibrium conditions and adop-ted therein the predicted α-helical conformation. Following a pattern similar to that previously described for HIV PreTM$_p$,

the presence of the raft-associated lipid sphingomyelin did not affect membrane insertion, but it stimulated highly the membrane-destabilizing capacity of Ebola PreTM$_p$. The SPM effect seemed to not arise from an intrinsic instability of the vesicles, since the scrambled control sequence could not induce leakage at any tested dose even though it interacted with liposomes. The outcome of this study underscored the importance of residue distribution within the Ebola PreTM sequence, specifically for the induction of membrane perturbations.

WW hydrophobicity analyses also put forward the existence of FP and PreTM-like membrane-transferring domains in SARS-CoV S sequence [38–40]. Membrane interactions of S2 PreTM-representative KYEQYIKWPWYVW peptide were subsequently characterized by means of CD, as well as in lipid vesicle permeabilization assays [39]. Even though the structural analyses indicated a low propensity for a defined secondary structure, S2 PreTM$_p$ strongly partitioned into lipid membranes and induced lipid vesicle permeabilization at peptide-to-lipid mol ratios of 1:100. It was found that a scrambled YEWKWIY-WYPVKQ peptide was severely impaired in its capacity to induce vesicle permeabilization. Thus, partitioning of the wild-type peptides into the lipid interface was sufficient to specifically disorganize membrane integrity. A mechanism was proposed according to which CoV S PreTM, aligned with the FP and TMD during membrane apposition, would function to perturb the target cell membrane, and also to provide a continuous track of hydrophobic surface. Assembly of this structure would result in lipid-membrane fusion and subsequent viral nucleocapsid entry.

A combined KD and WW analysis was also employed to unravel Herpes simplex virus type-1 (HSV-1) glycoprotein H (gH) sequences showing propensity to interact with membrane interfaces [69,70]. A putative helical membrane-interacting domain was identified just preceding the gH TMD [70]. A collection of HSV-1 gH PreTM$_p$-s was synthesized and characterized. It was found that STALLLFPNGTVIHLLAFDTQPVAAIA (designated as pTM5) induced fusion of PC/cholesterol-containing phospholipid vesicles, while SHVLTAPALTFNLTDFVPILALA-GIQA, a scrambled version with same amino acid composition, was defective in that activity. Interestingly, fusion activity in this case was related to the capacity of the PreTM$_p$ wild-type to adopt a β structure in contact with membranes. It was concluded that, similar to amino-terminal FPs, structural flexibility, rather than the rigid adoption of a particular secondary structure, might be a key property of the HSV-1 PreTM domain as a fusogen.

5. Interfacial domains in viral membrane fission

Completion of the newly assembled virions budding at cell membranes, known as "pinching-off" step, requires membrane fission [71–73]. Conformational energy release occurs in this case accompanied by multimerization of capsid proteins into spherical surfaces that grow in contact with the internal membrane monolayer. As one of the best-studied examples, Gag polyprotein is the main responsible for budding of immature HIV-1 particles, a process involving a complex interplay between viral and cell-host factors [1,2,72,74]. Gag-membrane association proceeds via the

N-terminal myristoyl moiety of matrix (MA) domain coupled to surface oligomerization [75–77]. Thus, Gag-membrane association and assembly therein are likely to promote each other, thereby driving the budding process.

Similarly, the minimal components needed to initiate, drive, and complete the Rhabdovirus budding process are the condensed RNP core in association with the matrix (M) protein [78]. However, in this case, in the absence of virally encoded glycoproteins the number of virus particles released from infected cells is significantly less than that made by WT virus. Therefore, the envelope glycoprotein contributes to virus egress. Involvement of VSV G PreTM in this process was studied using a series of recombinant Δ*G*-VSVs expressing chimeric glycoproteins with truncated stem sequences [67]. The recombinant viruses having chimeras with 12 or more PreTM residues, and including the G protein transmembrane-cytoplasmic tail domains, produced near-wild-type levels of particles. In contrast, viruses encoding chimeras with shorter or no PreTM sequences produced ca. 10- to 20-fold less. In line with its putative association with the membrane interface, these authors suggested that the VSV G PreTM might promote virus release by inducing positive membrane curvature at sites where virus budding occurs.

Alphavirus 6K protein provides a further opportunity for the study of interfacial domain activity in fission: firstly, this small protein's sequence comprises a single PreTM-TMD motif [79], and, secondly, 6K is not required for alphavirus budding, but catalyzes the process [80], which allows recovery of budding defective, but still infectious particles, upon cell transfection with alphaviral replicon.

The budding of alphavirus particles is essentially promoted by interaction of assembled nucleocapsids with the carboxy domain of envelope glycoprotein E2 [73,81]. Despite the association of the 6K protein with the plasma membrane and its interaction with E1–E2 glycoproteins, very little 6K is incorporated into the budded virus particles. The N-terminal 6K ectodomain encompasses two hydrophobic-at-interface segments that can mediate association of this sequence with the external membrane monolayer [79]. Conservation of the interfacial 6K segments among divergent members of the Alphavirus genus suggested a functional role for these motifs. Accordingly, Sindbis virus (SV) 6K variants that contained substitutions interfering with the capacity of the N-terminus to partition into membranes without affecting KD hydrophobicity were obtained and characterized. Electron microscopy of cells transfected with these mutants disclosed accumulation at the plasma membrane of otherwise morphologically normal virus particles, suggesting that mutations introduced in the interfacial 6K sequence resulted in impaired virus budding, likely due to inefficient pinching-off of the assembled virus particles.

6. PreTM domains as targets for viral fusion inhibition

Since entry inhibition may block early stages of viral infection, the large conformational changes that are the energy source for membrane fusion constitute an important target in development of antiviral therapies. A paradigmatic case is that of the

human immunodeficiency virus, (HIV). The HIV fusion inhibitor T-20 (enfuvirtide) is currently in use within the context of rescue therapies active against multidrug resistant viruses [82]. This peptidic compound dominantly competes with gp41 helical sequences for binding to hydrophobic grooves transiently exposed at the ectodomain surface [83,84]. Thus, it is postulated that T-20 blocks close contact between cell target and viral membranes by preventing 6-HB formation.

In principle the functional domains that transmit 6-HB formation energy into membranes, such as FP or PreTM, may constitute alternative targets for antiviral development. Compelling evidence that sustains suitability of FP function as a target for inhibitor development has been again obtained in the case of HIV-1. Early studies showed that oligopeptides homologous in sequence to the FP were indeed capable of inhibiting gp41-induced fusion [85–88]. Also supporting this view we have recently identified gp41 inhibitors from a D-amino acid hexapeptide library, based on their capacity to block synthetic FP_p in vitro [89], and Munch et al. [90] have isolated a naturally produced oligopeptide targeting FP that was able to block HIV-1 infection. Thus, force-transmitting sequences emerge as alternative therapeutic targets [90,91].

The ability displayed by HIV-1 $PreTM_p$ to self-associate in solution and membranes raised the possibility of PreTM homo-oligomer formation at some stage during gp41-induced fusion process [21,54]. It was inferred that PreTM homo-oligomer formation might represent a target for potential inhibitors. This hypothesis was tested analyzing $PreTM_p$ ability to interfere with cell–cell fusion induced by HIV-1 envelope [21]. HIV-1 $PreTM_p$ inhibited gp41-induced fusion in a dose-dependent manner with an apparent IC_{50} value of 577 nM. A W(1–3)A mutant-like peptide unable to form homo-oligomers was used as negative control and shown to be devoid of inhibitory effect. In control experiments, neither of these two peptides inhibited influenza hemagglutinin-mediated fusion implying that $PreTM_p$ inhibitory effect was through its interaction with HIV envelope protein, and not through its partitioning into cell membranes and causing non-specific perturbations.

As mentioned before, a cognate 20-mer peptide derived from FIV transmembrane glycoprotein PreTM, potently inhibited viral infectivity in tissue culture ($IC_{50} \approx 4$ nM) [66,92,93]. Antiviral activity of the leading PreTM sequence was found to map to a short segment containing three conserved Trp residues. Thus, further analyses focused on a derivative of eight amino acids (770WEDWVRWI777), designated C8, which still displayed potent antiviral activity ($IC_{50} \approx 40$ nM). C8 activity was found to be dependent on conservation of the Trp motif, most likely because these residues are responsible for its conformational propensity. Furthermore, the retroinverso analogue of this peptide (riC8) was shown to be effective *in vivo*, in experiments demonstrating its ability to decrease mean viral load when administered to chronically FIV-infected cats [92].

Albeit with an apparent lower affinity, peptides analogous to the S2 subunit PreTM domain inhibited SARS-CoV plaque formation (inhibition by 40–70% at concentrations of 15–30 μM) [94]. In line with these observations, HSV gH PreTM-derived pTM4 and pTM5 peptides, modified by addition of a tail

of lysine residues, were able to induce almost 100% inhibition of HSV-1 infectivity at concentrations in the range of 100 μM [70]. Underscoring the specificity of the observed effect, the scrambled version of pTM5 failed to inhibit infectivity under similar experimental conditions.

7. PreTM domains as targets for viral neutralization

Only two broadly neutralizing anti-HIV-1 antibodies isolated from peripheral blood mononuclear cells of HIV infected non-symptomatic patients have been described to react with gp41 [95,96]. These antibodies, designated as 2F5 and 4E10, recognize epitopes within the conserved PreTM domain (reviewed in Refs. [97–99], see also Fig. 1). 2F5 (662ELDKWAS668) and 4E10 (671NWFNIT676) core epitopes roughly span AIS and the junction between the two PreTM interfacial subdomains, respectively. Both of them have developed paratopes capable of inserting into membrane interfaces, which putatively enables them for recognition of membrane-inserted epitope sequences [50,99–102]. Recent experimental work by our group sustains specific recognition and blocking at membrane interfaces by both antibodies [100,103], although following different molecular mechanisms.

2F5 epitope appears to be an intrinsically flexible sequence with access to different conformations depending on the molecular context [34,104–109]. Crystallographic analysis of the 656NEQELLELDKWASLWN671 sequence in complex with Fab 2F5 displays an extended conformation at the amino-terminus, followed by two consecutive type I β-turns, which is assumed to represent a defined, native-like gp41 structure [101]. Thus, it is inferred that Mab2F5 will recognize with lower affinity the α-helical conformation adopted by AIS upon partitioning into the membrane interface [100]. In contrast, 4E10 antibody binds PreTM epitope in the helical conformation that is also stable at membrane interfaces [50,110,111] (Fig. 3).

MAb4E10 binding to the membrane-inserted epitope is reflected by its capacity of blocking $PreTM_p$-induced membrane-restructuring effects (Fig. 5 and Ref. [103]). The fact that membrane-restructuring blocking was dependent on the presence of Chol suggests an adaptation of 4E10 antibody for recognition of PreTM species residing at the virion external membrane interface [103]. In contrast, 4E10 did not greatly affect $PreTM_p$-induced perturbations in PC:SPM vesicles, most likely because $PreTM_p$ surface gets occluded in the transmembrane pores responsible for permeabilization of this type of vesicles [54,103]. Recognition at membrane interfaces was also made evident by fluorescence microscopy of lipid monolayers transferred onto glass coverslips [103]. In these experiments, addition of Mab4E10 was shown to induce surface clustering of $PreTM_p$ sequence in presence of Chol, but not in its absence. It was concluded that a putative mechanism of gp41 blocking might be based on Mab4E10 capacity for rendering cross-linked spikes incompetent for fusion.

In summary, adopted conformation, aggregation state and topology as affected by the envelope lipids may condition Mab4E10 recognition of membrane-inserted PreTM epitope.

8. Concluding remarks

In principle we cannot exclude the possibility that PreTM folds as a component of globular ectodomains, either during synthesis or at some stage before protein activation [112]. More likely, PreTM is recruited into the 6-HB during progression of the reaction mediated by class I fusion proteins. The observation that 2F5 and 4E10 epitopes disappear concomitant to fusion [113], i.e., coupled to 6-HB completion [114], would sustain this notion in the case of HIV-1 gp41. In fact, Mab2F5 recognizes its epitope with lower affinity in the context of synthetic 6-HB versions [115]. Thus, the absence of activity observed in cell–cell fusion assays upon complete gp41 PreTM ablation probably originates from the incapacity for coupling 6-HB formation to membrane merger [45,65].

However, as disclosed by WW analyses, membrane-inserted PreTM states exist with high probability (Fig. 1), a prediction that seems to fulfill for native HIV Env glycoproteins incorporated into virions [36,37]. In the context of cells expressing PreTM motifs, membrane-inserted PreTM states appear not to be absolutely required for initiation and progression of fusion or fission, their functional relevance being circumscribed to an assisting effect on those processes. In support of this view, a HIV-1 gp41 devoid of PreTM interfacial hydrophobicity is still competent in opening small fusion pores [45] (see also Fig. 2), ΔG-VSV is capable of inducing hemifusion on its own and also of functioning as a potentiator of fusion induced by other viral glycolproteins [68], and SV 6K catalyzes budding by promoting the pinching-off step [79].

Differential surface increase of the external membrane monolayer upon insertion might provide a common molecular mechanism to explain these catalytic effects [1,2]. Monolayer surface imbalance might contribute to membrane deformation and bending (positive curvature) at the points of virus budding. It is inferred that imparting positive curvature to distal *trans*-monolayers engaged in pinching-off will promote completion of the process [1,116]. More difficult to envisage is how positive curvature applied to contacting *cis*-monolayers might promote fusion. A possibility is that fusion is actually restrained by PreTM-induced positive curvature (committed state) until the process is activated. In such a case, extracting PreTM out of the interface, for instance by recruiting it into the growing 6-HB structure, might differentially reduce the surface of contacting monolayers, thereby stimulating fusion.

More specific structural and functional roles that might explain the high degree of HIV-1 PreTM sequence conservation, can be related to assembly, maturation and fusion activation of virions. These roles are likely to depend on its folding as an interfacial α-helix, which binds Chol, self-assembles in a raft environment, and is endowed with the capacity of restructuring this type of membranes. Indeed, most if not all PreTM mutants described by Salzwedel et al. dramatically affected incorporation of glycoprotein into virions [44]. These authors were the first to propose that one possible role for the conserved tryptophan residues in enhancing the incorporation of glycoprotein into virions could involve an interaction with cholesterol. Subsequently reported experimental evidence supports this notion [61–64]. Such interactions could facilitate the enrichment of glycoprotein within plasma membrane raft-domains through which the virus might bud [59], or even be employed in generating Chol-rich domains [62,117]. Thus, PreTM might function as a raft-sensor to pilot Env protein to budding sites during viral assembly. Furthermore, specific folding and self-association within a Chol-enriched raft environment might be crucial for gp41 function [56,118–121].

The low spike density existing in the virion envelope (≈ 10–20 spikes and $\approx 300,000$ lipids, see Refs. [35,58]) might in part account for HIV-1 PreTM sequence conservation. It is tempting to speculate that clusters of inserted PreTMs might be initially responsible for the induction of local positive curvature within laterally segregated areas of the external viral membrane monolayer. As a matter of fact, electron tomography of intact virions reveals spikes distributed forming clusters of at least seven members [36], and clusters of rod-shaped proteins at the focal points where the actual membrane merger develops [122]. Within these distinct areas, monolayer intrinsic curvatures could hypothetically change their sign upon PreTM desorption, thus facilitating fusion pore opening.

An alternative not exclusive option is that PreTM acts as an FP-like fusogenic sequence in laterally segregated PC-Chol domains, by promoting and/or stabilizing fusion pore architecture [29,30,123]. Sustaining this notion HIV-1 PreTM$_p$ partitions into POPC or POPC:SPM membranes but is only fusogenic when Chol is added to the lipid composition (Fig. 4 and Ref. [54]). Chol requirement actually supports that the membrane-restructuring processes observed in liposomes are indeed bona fide reflection of a gp41 PreTM physiological role [118,121] (Fig. 4). Moreover, PreTM$_p$ membrane activity is affected by blocking mutations (Fig. 2), occurs at membrane doses relevant for spike density (Fig. 4) and is inhibited by neutralizing antibodies (Fig. 5). Attending to data reported in the literature, such an intrinsic membrane-perturbing activity could be a general feature of viral PreTMs [21,29–31,39–41, 54,60,70,79,124–126]. However, structure–function requirements may vary depending on the virus family, and adoption of an interfacial helical conformation seems not to be a prerequisite for membrane-disruption induced by the different PreTM$_p$-s [30,39,70,124].

The close proximity to the membrane surface of TMD-linked PreTM implies an effective concentration high enough as to push partitioning equilibrium towards membrane-inserted species. Even for sequences that are not specially enriched in aromatic residues, a mild degree of hydrophobicity together with access to a defined secondary structure upon partitioning, is likely to suffice for stable insertion into the membrane interface. Thus, there arises the question of long aromatic-rich PreTM domains as representing an adaptive improvement in the context of viral infection strategies. Again, HIV-1 provides an example of the way this adaptation might operate.

Most surface of native gp41 in virions remains inaccessible to neutralizing antibodies due to steric occlusion by surface gp120 subunit and/or homo-oligomerization [97–99]. Just the MPER stem region is potentially exposed to solvent [112,127]. Thus, the probability of neutralization by binding to MPER

epitopes might be reduced by two complementary mechanisms: i) limiting the envelope spike number (i.e., reduction of binding-sites and concomitant avidity decrease), and ii) occluding MPER epitopes into the interface of the viral external membrane monolayer (affinity decrease). Long aromatic-rich PreTM might play a central role in driving both effects. In one hand, as discussed before, its capacity to self-associate at the raft-like membrane surface would buttress the reduction of the number of spikes at the viral surface required for fusion. On the other, its high degree of hydrophobicity-at-interface ensures embedding of stem epitope sequences into the membrane, thereby occluding key residues for recognition and/or inducing membrane-specific secondary structure.

Indeed, insertion into membrane interfaces, and even phospholipid recognition therein, have been postulated to correlate with the broadly neutralizing capacity of anti-gp41 2F5 and 4E10 antibodies [128–132]. Mab4E10 is capable of binding and blocking PreTM$_p$ in membranes at peptide-to-lipid ratios relevant for the low spike virion density [100,102,103]. We have proposed a mechanism of neutralization by 4E10 based on its capacity to cross-link interfacial PreTM sequences [103]. According to that mechanism 4E10 would disorganize the spike clusters required for fusion initiation. Further studies of the mechanisms governing membrane-inserted epitope recognition will lead to new insights regarding the know-how to design effective anti-HIV-1 vaccines.

9. Note added to proofs

The structure recently reported by Sun et al. (Immunity 28 (2008), 52-63) supports the bipartite nature of HIV-1 AIS-PreTM inserted at the membrane interface.

Acknowledgements

References

[1] L.V. Chernomordik, M.M. Kozlov, Protein-lipid interplay in fusion and fission of biological membranes, Annu. Rev. Biochem. 72 (2003) 175–207.

[2] W.B. Huttner, J. Zimmerberg, Implications of lipid microdomains for membrane curvature, budding and fission, Curr. Opin. Cell Biol. 13 (2001) 478–484.

[3] L.J. Earp, S.E. Delos, H.E. Park, J.M. White, The many mechanisms of viral membrane fusion proteins, Curr. Top. Microbiol. Immunol. 285 (2005) 25–66.

[4] D.J. Schibli, W. Weissenhorn, Class I and class II viral fusion protein structures reveal similar principles in membrane fusion, Mol. Membr. Biol. 21 (2004) 361–371.

[5] S.A. Gallo, C.M. Finnegan, M. Viard, Y. Raviv, A. Dimitrov, S.S. Rawat, A. Puri, S. Durell, R. Blumenthal, The HIV Env-mediated fusion reaction, Biochim. Biophys. Acta 1614 (2003) 36–50.

[6] J.J. Skehel, D.C. Wiley, Receptor binding and membrane fusion in virus entry: the influenza hemagglutinin, Annu. Rev. Biochem. 69 (2000) 531–569.

[7] J.M. White, Membrane fusion, Science 258 (1992) 917–924.

[8] M.J. Aman, C.M. Bosio, R.G. Panchal, J.C. Burnett, A. Schmaljohn, S. Bavari, Molecular mechanisms of filovirus cellular trafficking, Microbes Infect. 5 (2003) 639–649.

[9] J. Krijnse-Locker, B. Sodeik, M. Suomalainen, Meeting report from the EMBO workshop "The Cell Biology of Virus Infection", Heidelberg, Germany, 22–26 September 2001, Traffic 3 (2002) 233–235.

[10] J. Zimmerberg, S.S. Vogel, L.V. Chernomordik, Mechanisms of membrane fusion, Annu. Rev. Biophys. Biomol. Struct. 22 (1993) 433–466.

[11] B.R. Lentz, V. Malinin, M.E. Haque, K. Evans, Protein machines and lipid assemblies: current views of cell membrane fusion, Curr. Opin. Struct. Biol. 10 (2000) 607–615.

[12] G. Basanez, Membrane fusion: the process and its energy suppliers, Cell. Mol. Life Sci. 59 (2002) 1478–1490.

[13] J. Zimmerberg, K. Gawrisch, The physical chemistry of biological membranes, Nat. Chem. Biol. 2 (2006) 564–567.

[14] R. Blumenthal, M.J. Clague, S.R. Durell, R.M. Epand, Membrane fusion, Chem. Rev. 103 (2003) 53–69.

[15] W. Weissenhorn, A. Hinz, Y. Gaudin, Virus membrane fusion, FEBS Lett. 581 (2007) 2150–2155.

[16] S.R. Durell, I. Martin, J.M. Ruysschaert, Y. Shai, R. Blumenthal, What studies of fusion peptides tell us about viral envelope glycoprotein-mediated membrane fusion (review), Mol. Membr. Biol. 14 (1997) 97–112.

[17] R.M. Epand, Fusion peptides and the mechanism of viral fusion, Biochim. Biophys. Acta 1614 (2003) 116–121.

[18] J.L. Nieva, A. Agirre, Are fusion peptides a good model to study viral cell fusion? Biochim. Biophys. Acta 1614 (2003) 104–115.

[19] D.L. Gibbons, M.C. Vaney, A. Roussel, A. Vigouroux, B. Reilly, J. Lepault, M. Kielian, F.A. Rey, Conformational change and protein–protein interactions of the fusion protein of Semliki Forest virus, Nature 427 (2004) 320–325.

[20] S.G. Peisajovich, Y. Shai, Viral fusion proteins: multiple regions contribute to membrane fusion, Biochim. Biophys. Acta 1614 (2003) 122–129.

[21] A. Saez-Cirion, J.L. Arrondo, M.J. Gomara, M. Lorizate, I. Iloro, G. Melikyan, J.L. Nieva, Structural and functional roles of HIV-1 gp41 pretransmembrane sequence segmentation, Biophys. J. 85 (2003) 3769–3780.

[22] J.L. Nieva, T. Suarez, Hydrophobic-at-interface regions in viral fusion protein ectodomains, Biosci. Rep. 20 (2000) 519–533.

[23] W.C. Wimley, S.H. White, Experimentally determined hydrophobicity scale for proteins at membrane interfaces, Nat. Struct. Biol. 3 (1996) 842–848.

[24] S.H. White, W.C. Wimley, Membrane protein folding and stability: physical principles, Annu. Rev. Biophys. Biomol. Struct. 28 (1999) 319–365.

[25] F.B. Pereira, F.M. Goni, A. Muga, J.L. Nieva, Permeabilization and fusion of uncharged lipid vesicles induced by the HIV-1 fusion peptide adopting an extended conformation: dose and sequence effects, Biophys. J. 73 (1997) 1977–1986.

[26] M.B. Ruiz-Arguello, F.M. Goni, F.B. Pereira, J.L. Nieva, Phosphatidylinositol-dependent membrane fusion induced by a putative fusogenic sequence of Ebola virus, J. Virol. 72 (1998) 1775–1781.

[27] S. Nir, J.L. Nieva, Interactions of peptides with liposomes: pore formation and fusion, Prog. Lipid Res. 39 (2000) 181–206.

[28] J. Kyte, R.F. Doolittle, A simple method for displaying the hydropathic character of a protein, J. Mol. Biol. 157 (1982) 105–132.

[29] T. Suarez, W.R. Gallaher, A. Agirre, F.M. Goni, J.L. Nieva, Membrane interface-interacting sequences within the ectodomain of the human immunodeficiency virus type 1 envelope glycoprotein: putative role during viral fusion, J. Virol. 74 (2000) 8038–8047.

[30] T. Suarez, S. Nir, F.M. Goni, A. Saez-Cirion, J.L. Nieva, The pre-transmembrane region of the human immunodeficiency virus type-1 glycoprotein: a novel fusogenic sequence, FEBS Lett. 477 (2000) 145–149.

[31] A. Saez-Cirion, M.J. Gomara, A. Agirre, J.L. Nieva, Pre-transmembrane sequence of Ebola glycoprotein. Interfacial hydrophobicity distribution and interaction with membranes, FEBS Lett. 533 (2003) 47–53.

[32] D. Eisenberg, R.M. Weiss, T.C. Terwilliger, The helical hydrophobic moment: a measure of the amphiphilicity of a helix, Nature 299 (1982) 371–374.

[33] D. Eisenberg, R.M. Weiss, T.C. Terwilliger, The hydrophobic moment detects periodicity in protein hydrophobicity, Proc. Natl. Acad. Sci. U. S. A. 81 (1984) 140–144.

[34] M. Lorizate, I. de la Arada, N. Huarte, S. Sanchez-Martinez, B.G. de la Torre, D. Andreu, J.L. Arrondo, J.L. Nieva, Structural analysis and assembly of the HIV-1 Gp41 amino-terminal fusion peptide and the pretransmembrane amphipathic-at-interface sequence, Biochemistry 45 (2006) 14337–14346.

[35] P. Zhu, E. Chertova, J. Bess Jr., J.D. Lifson, L.O. Arthur, J. Liu, K.A. Taylor, K.H. Roux, Electron tomography analysis of envelope glycoprotein trimers on HIV and simian immunodeficiency virus virions, Proc. Natl. Acad. Sci. U. S. A. 100 (2003) 15812–15817.

[36] P. Zhu, J. Liu, J. Bess Jr., E. Chertova, J.D. Lifson, H. Grise, G.A. Ofek, K.A. Taylor, K.H. Roux, Distribution and three-dimensional structure of AIDS virus envelope spikes, Nature 441 (2006) 847–852.

[37] K.H. Roux, K.A. Taylor, AIDS virus envelope spike structure, Curr. Opin. Struct. Biol. 17 (2007) 244–252.

[38] B. Sainz Jr., J.M. Rausch, W.R. Gallaher, R.F. Garry, W.C. Wimley, Identification and characterization of the putative fusion peptide of the severe acute respiratory syndrome-associated coronavirus spike protein, J. Virol. 79 (2005) 7195–7206.

[39] B. Sainz Jr., J.M. Rausch, W.R. Gallaher, R.F. Garry, W.C. Wimley, The aromatic domain of the coronavirus class I viral fusion protein induces membrane permeabilization: putative role during viral entry, Biochemistry 44 (2005) 947–958.

[40] J. Guillen, A.J. Perez-Berna, M.R. Moreno, J. Villalain, Identification of the membrane-active regions of the severe acute respiratory syndrome coronavirus spike membrane glycoprotein using a 16/18-mer peptide scan: implications for the viral fusion mechanism, J. Virol. 79 (2005) 1743–1752.

[41] S. Giannecchini, F. Bonci, M. Pistello, D. Matteucci, O. Sichi, P. Rovero, M. Bendinelli, The membrane-proximal tryptophan-rich region in the transmembrane glycoprotein ectodomain of feline immunodeficiency virus is important for cell entry, Virology 320 (2004) 156–166.

[42] H. Garg, F.J. Fuller, W.A. Tompkins, Mechanism of feline immunodeficiency virus envelope glycoprotein-mediated fusion, Virology 321 (2004) 274–286.

[43] E. Jeetendra, K. Ghosh, D. Odell, J. Li, H.P. Ghosh, M.A. Whitt, The membrane-proximal region of vesicular stomatitis virus glycoprotein G ectodomain is critical for fusion and virus infectivity, J. Virol. 77 (2003) 12807–12818.

[44] K. Salzwedel, J.T. West, E. Hunter, A conserved tryptophan-rich motif in the membrane-proximal region of the human immunodeficiency virus type 1 gp41 ectodomain is important for Env-mediated fusion and virus infectivity, J. Virol. 73 (1999) 2469–2480.

[45] I. Munoz-Barroso, K. Salzwedel, E. Hunter, R. Blumenthal, Role of the membrane-proximal domain in the initial stages of human immunodeficiency virus type 1 envelope glycoprotein-mediated membrane fusion, J. Virol. 73 (1999) 6089–6092.

[46] R.M. Markosyan, F.S. Cohen, G.B. Melikyan, The lipid-anchored ectodomain of influenza virus hemagglutinin (GPI-HA) is capable of inducing nonenlarging fusion pores, Mol. Biol. Cell 11 (2000) 1143–1152.

[47] S.H. White, A.S. Ladokhin, S. Jayasinghe, K. Hristova, How membranes shape protein structure, J. Biol. Chem. 276 (2001) 32395–32398.

[48] N. Sal-Man, D. Gerber, I. Bloch, Y. Shai, Specificity in transmembrane helix–helix interactions mediated by aromatic residues, J. Biol. Chem. 282 (2007) 19753–19761.

[49] D.J. Schibli, R.C. Montelaro, H.J. Vogel, The membrane-proximal tryptophan-rich region of the HIV glycoprotein, gp41, forms a well-defined helix in dodecylphosphocholine micelles, Biochemistry 40 (2001) 9570–9578.

[50] R.M. Cardoso, M.B. Zwick, R.L. Stanfield, R. Kunert, J.M. Binley, H. Katinger, D.R. Burton, I.A. Wilson, Broadly neutralizing anti-HIV antibody 4E10 recognizes a helical conformation of a highly conserved fusion-associated motif in gp41, Immunity 22 (2005) 163–173.

[51] A.E. Keating, V.N. Malashkevich, B. Tidor, P.S. Kim, Side-chain repacking calculations for predicting structures and stabilities of heterodimeric coiled coils, Proc. Natl. Acad. Sci. U. S. A. 98 (2001) 14825–14830.

[52] J.R. Litowski, R.S. Hodges, Designing heterodimeric two-stranded alpha-helical coiled-coils. Effects of hydrophobicity and alpha-helical propensity on protein folding, stability, and specificity, J. Biol. Chem. 277 (2002) 37272–37279.

[53] K. Park, A. Perczel, G.D. Fasman, Differentiation between transmembrane helices and peripheral helices by the deconvolution of circular dichroism spectra of membrane proteins, Protein Sci. 1 (1992) 1032–1049.

[54] A. Saez-Cirion, S. Nir, M. Lorizate, A. Agirre, A. Cruz, J. Perez-Gil, J.L. Nieva, Sphingomyelin and cholesterol promote HIV-1 gp41 pretransmembrane sequence surface aggregation and membrane restructuring, J. Biol. Chem. 277 (2002) 21776–21785.

[55] W.C. Reisdorf Jr., S. Krimm, Infrared amide I' band of the coiled coil, Biochemistry 35 (1996) 1383–1386.

[56] R.C. Aloia, F.C. Jensen, C.C. Curtain, P.W. Mobley, L.M. Gordon, Lipid composition and fluidity of the human immunodeficiency virus, Proc. Natl. Acad. Sci. U. S. A. 85 (1988) 900–904.

[57] R.C. Aloia, H. Tian, F.C. Jensen, Lipid composition and fluidity of the human immunodeficiency virus envelope and host cell plasma membranes, Proc. Natl. Acad. Sci. U. S. A. 90 (1993) 5181–5185.

[58] B. Brugger, B. Glass, P. Haberkant, I. Leibrecht, F.T. Wieland, H.G. Krausslich, The HIV lipidome: a raft with an unusual composition, Proc. Natl. Acad. Sci. U. S. A. 103 (2006) 2641–2646.

[59] D.H. Nguyen, J.E. Hildreth, Evidence for budding of human immunodeficiency virus type 1 selectively from glycolipid-enriched membrane lipid rafts, J. Virol. 74 (2000) 3264–3272.

[60] S. Shnaper, K. Sackett, S.A. Gallo, R. Blumenthal, Y. Shai, The C- and the N-terminal regions of glycoprotein 41 ectodomain fuse membranes enriched and not enriched with cholesterol, respectively, J. Biol. Chem. 279 (2004) 18526–18534.

[61] N. Vincent, C. Genin, E. Malvoisin, Identification of a conserved domain of the HIV-1 transmembrane protein gp41 which interacts with cholesteryl groups, Biochim. Biophys. Acta 1567 (2002) 157–164.

[62] R.F. Epand, B.G. Sayer, R.M. Epand, The tryptophan-rich region of HIV gp41 and the promotion of cholesterol-rich domains, Biochemistry 44 (2005) 5525–5531.

[63] R.F. Epand, A. Thomas, R. Brasseur, S.A. Vishwanathan, E. Hunter, R.M. Epand, Juxtamembrane protein segments that contribute to recruitment of cholesterol into domains, Biochemistry 45 (2006) 6105–6114.

[64] R.M. Epand, Cholesterol and the interaction of proteins with membrane domains, Prog. Lipid Res. 45 (2006) 279–294.

[65] A.S. Dimitrov, S.S. Rawat, S. Jiang, R. Blumenthal, Role of the fusion peptide and membrane-proximal domain in HIV-1 envelope glycoprotein-mediated membrane fusion, Biochemistry 42 (2003) 14150–14158.

[66] S. Giannecchini, A. Di Fenza, A.M. D'Ursi, D. Matteucci, P. Rovero, M. Bendinelli, Antiviral activity and conformational features of an octapeptide derived from the membrane-proximal ectodomain of the feline immunodeficiency virus transmembrane glycoprotein, J. Virol. 77 (2003) 3724–3733.

[67] C.S. Robison, M.A. Whitt, The membrane-proximal stem region of vesicular stomatitis virus G protein confers efficient virus assembly, J. Virol. 74 (2000) 2239–2246.

[68] E. Jeetendra, C.S. Robison, L.M. Albritton, M.A. Whitt, The membrane-proximal domain of vesicular stomatitis virus G protein functions as a membrane fusion potentiator and can induce hemifusion, J. Virol. 76 (2002) 12300–12311.

[69] S. Galdiero, A. Falanga, M. Vitiello, H. Browne, C. Pedone, M. Galdiero, Fusogenic domains in herpes simplex virus type 1 glycoprotein H, J. Biol. Chem. 280 (2005) 28632–28643.

[70] S. Galdiero, A. Falanga, M. Vitiello, M. D'Isanto, C. Collins, V. Orrei, H. Browne, C. Pedone, M. Galdiero, Evidence for a role of the membrane-proximal region of herpes simplex virus Type 1 glycoprotein H in membrane fusion and virus inhibition, Chembiochem 8 (2007) 885–895.

[71] N. Chazal, D. Gerlier, Virus entry, assembly, budding, and membrane rafts, Microbiol. Mol. Biol. Rev. 67 (2003) 226–237 table of contents.

[72] O. Pornillos, J.E. Garrus, W.I. Sundquist, Mechanisms of enveloped RNA virus budding, Trends Cell Biol. 12 (2002) 569–579.

[73] H. Garoff, R. Hewson, D.J. Opstelten, Virus maturation by budding, Microbiol. Mol. Biol. Rev. 62 (1998) 1171–1190.

[74] E.O. Freed, Viral late domains, J. Virol. 76 (2002) 4679–4687.

[75] A. Ono, J.M. Orenstein, E.O. Freed, Role of the Gag matrix domain in targeting human immunodeficiency virus type 1 assembly, J. Virol. 74 (2000) 2855–2866.

[76] D. Perez-Caballero, T. Hatziioannou, J. Martin-Serrano, P.D. Bieniasz, Human immunodeficiency virus type 1 matrix inhibits and confers cooperativity on gag precursor-membrane interactions, J. Virol. 78 (2004) 9560–9563.

[77] S. Sandefur, V. Varthakavi, P. Spearman, The I domain is required for efficient plasma membrane binding of human immunodeficiency virus type 1 Pr55Gag, J. Virol. 72 (1998) 2723–2732.

[78] H.R. Jayakar, E. Jeetendra, M.A. Whitt, Rhabdovirus assembly and budding, Virus Res. 106 (2004) 117–132.

[79] M.A. Sanz, V. Madan, L. Carrasco, J.L. Nieva, Interfacial domains in Sindbis virus 6K protein. Detection and functional characterization, J. Biol. Chem. 278 (2003) 2051–2057.

[80] P. Liljestrom, S. Lusa, D. Huylebroeck, H. Garoff, In vitro mutagenesis of a full-length cDNA clone of Semliki Forest virus: the small 6000-molecular-weight membrane protein modulates virus release, J. Virol. 65 (1991) 4107–4113.

[81] K.E. Owen, R.J. Kuhn, Alphavirus budding is dependent on the interaction between the nucleocapsid and hydrophobic amino acids on the cytoplasmic domain of the E2 envelope glycoprotein, Virology 230 (1997) 187–196.

[82] S.E. Schneider, B.L. Bray, C.J. Mader, P.E. Friedrich, M.W. Anderson, T.S. Taylor, N. Boshernitzan, T.E. Niemi, B.C. Fulcher, S.R. Whight, J.M. White, R.J. Greene, L.E. Stoltenberg, M. Lichty, Development of HIV fusion inhibitors, J. Pept. Sci. 11 (2005) 744–753.

[83] R.W. Doms, J.P. Moore, HIV-1 membrane fusion: targets of opportunity, J. Cell Biol. 151 (2000) F9–F14.

[84] D.M. Eckert, P.S. Kim, Mechanisms of viral membrane fusion and its inhibition, Annu. Rev. Biochem. 70 (2001) 777–810.

[85] R.J. Owens, C.C. Tanner, M.J. Mulligan, R.V. Srinivas, R.W. Compans, Oligopeptide inhibitors of HIV-induced syncytium formation, AIDS Res. Hum. Retrovir. 6 (1990) 1289–1296.

[86] V.A. Slepushkin, G.V. Kornilaeva, S.M. Andreev, M.V. Sidorova, A.O. Petrukhina, G.R. Matsevich, S.V. Raduk, V.B. Grigoriev, T.V. Makarova, V.V. Lukashov, et al., Inhibition of human immunodeficiency virus type 1 (HIV-1) penetration into target cells by synthetic peptides mimicking the N-terminus of the HIV-1 transmembrane glycoprotein, Virology 194 (1993) 294–301.

[87] Y. Kliger, A. Aharoni, D. Rapaport, P. Jones, R. Blumenthal, Y. Shai, Fusion peptides derived from the HIV type 1 glycoprotein 41 associate within phospholipid membranes and inhibit cell–cell fusion. Structure-function study, J. Biol. Chem. 272 (1997) 13496–13505.

[88] F.B. Pereira, F.M. Goni, J.L. Nieva, Membrane fusion induced by the HIV type 1 fusion peptide: modulation by factors affecting glycoprotein 41 activity and potential anti-HIV compounds, AIDS Res. Hum. Retrovir. 13 (1997) 1203–1211.

[89] M.J. Gomara, M. Lorizate, N. Huarte, I. Mingarro, E. Perez-Paya, J.L. Nieva, Hexapeptides that interfere with HIV-1 fusion peptide activity in liposomes block GP41-mediated membrane fusion, FEBS Lett. 580 (2006) 2561–2566.

[90] J. Munch, L. Standker, K. Adermann, A. Schulz, M. Schindler, R. Chinnadurai, S. Pohlmann, C. Chaipan, T. Biet, T. Peters, B. Meyer, D. Wilhelm, H. Lu, W. Jing, S. Jiang, W.G. Forssmann, F. Kirchhoff, Discovery and optimization of a natural HIV-1 entry inhibitor targeting the gp41 fusion peptide, Cell 129 (2007) 263–275.

[91] R. Blumenthal, D.S. Dimitrov, Targeting the sticky fingers of HIV-1, Cell 129 (2007) 243–245.

[92] S. Giannecchini, M.C. Alcaro, P. Isola, O. Sichi, M. Pistello, A.M. Papini, P. Rovero, M. Bendinelli, Feline immunodeficiency virus plasma load reduction by a retroinverso octapeptide reproducing the Trp-rich motif of the transmembrane glycoprotein, Antivir. Ther. 10 (2005) 671–680.

[93] S. Lombardi, C. Massi, E. Indino, C. La Rosa, P. Mazzetti, M.L. Falcone, P. Rovero, A. Fissi, O. Pieroni, P. Bandecchi, F. Esposito, F. Tozzini, M. Bendinelli, C. Garzelli, Inhibition of feline immunodeficiency virus infection in vitro by envelope glycoprotein synthetic peptides, Virology 220 (1996) 274–284.

[94] B. Sainz Jr., E.C. Mossel, W.R. Gallaher, W.C. Wimley, C.J. Peters, R.B. Wilson, R.F. Garry, Inhibition of severe acute respiratory syndrome-associated coronavirus (SARS-CoV) infectivity by peptides analogous to the viral spike protein, Virus Res. 120 (2006) 146–155.

[95] T. Muster, F. Steindl, M. Purtscher, A. Trkola, A. Klima, G. Himmler, F. Ruker, H. Katinger, A conserved neutralizing epitope on gp41 of human immunodeficiency virus type 1, J. Virol. 67 (1993) 6642–6647.

[96] G. Stiegler, R. Kunert, M. Purtscher, S. Wolbank, R. Voglauer, F. Steindl, H. Katinger, A potent cross-clade neutralizing human monoclonal antibody against a novel epitope on gp41 of human immunodeficiency virus type 1, AIDS Res. Hum. Retrovir. 17 (2001) 1757–1765.

[97] R. Wyatt, J. Sodroski, The HIV-1 envelope glycoproteins: fusogens, antigens, and immunogens, Science 280 (1998) 1884–1888.

[98] D.R. Burton, R.C. Desrosiers, R.W. Doms, W.C. Koff, P.D. Kwong, J.P. Moore, G.J. Nabel, J. Sodroski, I.A. Wilson, R.T. Wyatt, HIV vaccine design and the neutralizing antibody problem, Nat. Immunol. 5 (2004) 233–236.

[99] M.B. Zwick, The membrane-proximal external region of HIV-1 gp41: a vaccine target worth exploring, Aids 19 (2005) 1725–1737.

[100] S. Sanchez-Martinez, M. Lorizate, H. Katinger, R. Kunert, J.L. Nieva, Membrane association and epitope recognition by HIV-1 neutralizing anti-gp41 2F5 and 4E10 antibodies, AIDS Res. Hum. Retrovir. 22 (2006) 998–1006.

[101] G. Ofek, M. Tang, A. Sambor, H. Katinger, J.R. Mascola, R. Wyatt, P.D. Kwong, Structure and mechanistic analysis of the anti-human immunodeficiency virus type 1 antibody 2F5 in complex with its gp41 epitope, J. Virol. 78 (2004) 10724–10737.

[102] S.M. Alam, M. McAdams, D. Boren, M. Rak, R.M. Scearce, F. Gao, Z.T. Camacho, D. Gewirth, G. Kelsoe, P. Chen, B.F. Haynes, The role of antibody polyspecificity and lipid reactivity in binding of broadly neutralizing anti-HIV-1 envelope human monoclonal antibodies 2F5 and 4E10 to glycoprotein 41 membrane proximal envelope epitopes, J. Immunol. 178 (2007) 4424–4435.

[103] M. Lorizate, A. Cruz, N. Huarte, R. Kunert, J. Perez-Gil, J.L. Nieva, Recognition and blocking of HIV-1 gp41 pre-transmembrane sequence by monoclonal 4E10 antibody in a Raft-like membrane environment, J. Biol. Chem. 281 (2006) 39598–39606.

[104] G. Barbato, E. Bianchi, P. Ingallinella, W.H. Hurni, M.D. Miller, G. Ciliberto, R. Cortese, R. Bazzo, J.W. Shiver, A. Pessi, Structural analysis of the epitope of the anti-HIV antibody 2F5 sheds light into its mechanism of neutralization and HIV fusion, J. Mol. Biol. 330 (2003) 1101–1115.

[105] Z. Biron, S. Khare, S.R. Quadt, Y. Hayek, F. Naider, J. Anglister, The 2F5 epitope is helical in the HIV-1 entry inhibitor T-20, Biochemistry 44 (2005) 13602–13611.

[106] Z. Biron, S. Khare, A.O. Samson, Y. Hayek, F. Naider, J. Anglister, A monomeric 3(10)-helix is formed in water by a 13-residue peptide representing the neutralizing determinant of HIV-1 on gp41, Biochemistry 41 (2002) 12687–12696.

[107] M. Lorizate, M.J. Gomara, B.G. de la Torre, D. Andreu, J.L. Nieva, Membrane-transferring sequences of the HIV-1 Gp41 ectodomain assemble into an immunogenic complex, J. Mol. Biol. 360 (2006) 45–55.

[108] G.B. McGaughey, M. Citron, R.C. Danzeisen, R.M. Freidinger, V.M. Garsky, W.M. Hurni, J.G. Joyce, X. Liang, M. Miller, J. Shiver, M.J. Bogusky, HIV-1 vaccine development: constrained peptide immunogens show improved binding to the anti-HIV-1 gp41 MAb, Biochemistry 42 (2003) 3214–3223.

[109] J.G. Joyce, W.M. Hurni, M.J. Bogusky, V.M. Garsky, X. Liang, M.P. Citron, R.C. Danzeisen, M.D. Miller, J.W. Shiver, P.M. Keller, Enhancement of alpha-helicity in the HIV-1 inhibitory peptide DP178 leads to an increased affinity for human monoclonal antibody 2F5 but does not elicit neutralizing responses in vitro. Implications for vaccine design, J. Biol. Chem. 277 (2002) 45811–45820.

[110] F.M. Brunel, M.B. Zwick, R.M. Cardoso, J.D. Nelson, I.A. Wilson, D.R. Burton, P.E. Dawson, Structure–function analysis of the epitope for 4E10, a broadly neutralizing human immunodeficiency virus type 1 antibody, J. Virol. 80 (2006) 1680–1687.

[111] R.M. Cardoso, F.M. Brunel, S. Ferguson, M. Zwick, D.R. Burton, P.E. Dawson, I.A. Wilson, Structural basis of enhanced binding of extended and helically constrained peptide epitopes of the broadly neutralizing HIV-1 antibody 4E10, J. Mol. Biol. 365 (2007) 1533–1544.

[112] G. Zanetti, J.A. Briggs, K. Grunewald, Q.J. Sattentau, S.D. Fuller, Cryo-electron tomographic structure of an immunodeficiency virus envelope complex in situ, PLoS Pathog. 2 (2006) e83.

[113] A.S. Dimitrov, A. Jacobs, C.M. Finnegan, G. Stiegler, H. Katinger, R. Blumenthal, Exposure of the membrane-proximal external region of HIV-1 gp41 in the course of HIV-1 envelope glycoprotein-mediated fusion, Biochemistry 46 (2007) 1398–1401.

[114] G.B. Melikyan, R.M. Markosyan, H. Hemmati, M.K. Delmedico, D.M. Lambert, F.S. Cohen, Evidence that the transition of HIV-1 gp41 into a six-helix bundle, not the bundle configuration, induces membrane fusion, J. Cell Biol. 151 (2000) 413–423.

[115] M.K. Gorny, S. Zolla-Pazner, Recognition by human monoclonal antibodies of free and complexed peptides representing the prefusogenic and fusogenic forms of human immunodeficiency virus type 1 gp41, J. Virol. 74 (2000) 6186–6192.

[116] L. Chernomordik, A. Chanturiya, J. Green, J. Zimmerberg, The hemifusion intermediate and its conversion to complete fusion: regulation by membrane composition, Biophys. J. 69 (1995) 922–929.

[117] R.M. Epand, Do proteins facilitate the formation of cholesterol-rich domains? Biochim. Biophys. Acta 1666 (2004) 227–238.

[118] S. Campbell, K. Gaus, R. Bittman, W. Jessup, S. Crowe, J. Mak, The raft-promoting property of virion-associated cholesterol, but not the presence of virion-associated Brij 98 rafts, is a determinant of human immunodeficiency virus type 1 infectivity, J. Virol. 78 (2004) 10556–10565.

[119] S.M. Campbell, S.M. Crowe, J. Mak, Virion-associated cholesterol is critical for the maintenance of HIV-1 structure and infectivity, Aids 16 (2002) 2253–2261.

[120] D.R. Graham, E. Chertova, J.M. Hilburn, L.O. Arthur, J.E. Hildreth, Cholesterol depletion of human immunodeficiency virus type 1 and simian immunodeficiency virus with beta-cyclodextrin inactivates and permeabilizes the virions: evidence for virion-associated lipid rafts, J. Virol. 77 (2003) 8237–8248.

[121] Z. Liao, D.R. Graham, J.E. Hildreth, Lipid rafts and HIV pathogenesis: virion-associated cholesterol is required for fusion and infection of susceptible cells, AIDS Res. Hum. Retrovir. 19 (2003) 675–687.

[122] R. Sougrat, A. Bartesaghi, J.D. Lifson, A.E. Bennett, J.W. Bess, D.J. Zabransky, S. Subramaniam, Electron tomography of the contact between T cells and SIV/HIV-1: implications for viral entry, PLoS Pathog. 3 (2007) e63.

[123] B.G. Tenchov, R.C. MacDonald, D.P. Siegel, Cubic phases in phosphatidylcholine–cholesterol mixtures: cholesterol as membrane "fusogen", Biophys. J. 91 (2006) 2508–2516.

[124] C. Esposito, G. D'Errico, M.R. Armenante, S. Giannecchini, M. Bendinelli, P. Rovero, A.M. D'Ursi, Physicochemical characterization of a peptide deriving from the glycoprotein gp36 of the feline immunodeficiency virus and its lipoylated analogue in micellar systems, Biochim. Biophys. Acta 1758 (2006) 1653–1661.

[125] P.W. Mobley, J.A. Barry, A.J. Waring, M.A. Sherman, L.M. Gordon, Membrane perturbing actions of HIV type 1 glycoprotein 41 domains are inhibited by helical C-peptides, AIDS Res. Hum. Retrovir. 23 (2007) 224–242.

[126] J.L. Nieva, M.A. Sanz, L. Carrasco, Membrane-permeabilizing motif in Semliki forest virus E1 glycoprotein, FEBS Lett. 576 (2004) 417–422.

[127] M.B. Zwick, A.F. Labrijn, M. Wang, C. Spenlehauer, E.O. Saphire, J.M. Binley, J.P. Moore, G. Stiegler, H. Katinger, D.R. Burton, P.W. Parren, Broadly neutralizing antibodies targeted to the membrane-proximal external region of human immunodeficiency virus type 1 glycoprotein gp41, J. Virol. 75 (2001) 10892–10905.

[128] B.F. Haynes, J. Fleming, E.W. St Clair, H. Katinger, G. Stiegler, R. Kunert, J. Robinson, R.M. Scearce, K. Plonk, H.F. Staats, T.L. Ortel, H.X. Liao, S.M. Alam, Cardiolipin polyspecific autoreactivity in two broadly neutralizing HIV-1 antibodies, Science 308 (2005) 1906–1908.

[129] Z. Beck, N. Karasavvas, J. Tong, G.R. Matyas, M. Rao, C.R. Alving, Calcium modulation of monoclonal antibody binding to phosphatidylinositol phosphate, Biochem. Biophys. Res. Commun. 354 (2007) 747–751.

[130] S. Sanchez-Martinez, M. Lorizate, K. Hermann, R. Kunert, G. Basanez, J.L. Nieva, Specific phospholipid recognition by human immunodeficiency virus type-1 neutralizing anti-gp41 2F5 antibody, FEBS Lett. 580 (2006) 2395–2399.

[131] C.R. Alving, Z. Beck, N. Karasavva, G.R. Matyas, M. Rao, HIV-1, lipid rafts, and antibodies to liposomes: implications for anti-viral-neutralizing antibodies, Mol. Membr. Biol. 23 (2006) 453–465.

[132] B.K. Brown, N. Karasavvas, Z. Beck, G.R. Matyas, D.L. Birx, V.R. Polonis, C.R. Alving, Monoclonal antibodies to phosphatidylinositol phosphate neutralize human immunodeficiency virus type 1: role of phosphate-binding subsites, J. Virol. 81 (2007) 2087–2091.